

# COMPUTATIONAL MODEL ANALYSIS FOR EXPERIMENTAL OBSERVATION OF OPTICAL CURRENT NOISE SUPPRESSION BELOW THE SHOT-NOISE LIMIT

A. Nause, E. Gover, Tel Aviv University, Israel

## Abstract

In this paper we present simulation analysis of experimental results which demonstrate noise suppression in the optical regime, for a relativistic e-beam, below the classical shot-noise limit. Shot-noise is a noise resulting from the granular nature of the space-charge in an e-beam. It is linear to the beam current due to its Poissonic distribution in the emission process. Plasma oscillations driven by collective Coulomb interaction during beam drift between the electrons of a cold intense beam are the source of the effect of current noise suppression. The effect was experimentally demonstrated [1] by measuring Optical Transition Radiation (OTR) power per unit e-beam pulse charge. The interpretation of these results is that the beam charge homogenizes due to the collective interaction (sub-Poissonian distribution) and therefore the spontaneous radiation emission from such a beam would also be suppressed (Dicke's sub-radiance [2]). Analysis of the experimental results using GPT simulations will demonstrate the suppression effect. For the simulation results we used a full 3D GPT model of the ATF section in which the experiment took place at.

## INTRODUCTION

Shot-noise is a noise resulting from the granular nature of the space-charge in an e-beam. The discreteness of the particles and the randomness of electrons emission from the cathode causes time dependent fluctuations of the charge and current density at any cross section along the beam transport line. This noise was first reported in 1918 by Schottky who made experiments in vacuum tubes.

Noise is best characterized in terms of the Fourier transform of the time-varying fluctuations in electric current, namely, by its spectral density. Gover and Dyunin showed in a 1D model [3] that it is possible to observe and control optical frequency energy and current (shot noise) fluctuations in a dense relativistic charged particles beam. GPT simulations were used to demonstrate this effect for a real-like beam starting from Shot-noise [4]. Moreover, at certain conditions, when the dominant noise in the beam is current shot noise (density fluctuations), it is possible to reduce significantly the beam noise by virtue of a collective interaction process along an interaction length corresponding to a quarter period longitudinal plasma oscillation in the beam. This means that the charge distribution in the beam can be homogenized in this process.

First experimental observation of this phenomenon using OTR from a metallic foil was presented last year [1]. Noise suppression using a dispersive section (dog-leg bend) was demonstrated in SLAC [5]. TR is proportional to the

current-noise amplitude [6], and therefore can be used in order to estimate the suppression in the current noise. In this paper we press analysis of the experimental results and demonstrate this effect using full 3D GPT simulations that were carried out for this purpose.

## 1D Model of Noise Dynamics in Charged Electron Beams

In electron-beam transport under appreciable space-charge conditions, the microdynamic noise evolution process may be viewed as the stochastic oscillations of Langmuir plasma waves [3]. In the linear regime, the evolution of longitudinal current and velocity modulations of a beam of average current  $I_b$ , velocity  $\beta c$  and energy  $E = (\gamma - 1)mc^2$ , can be described in the laboratory frame by [7]:

$$\frac{d}{d\phi_p} \check{i}(z, \omega) = -\frac{i}{W(z)\check{v}(z, \omega)} \quad (1)$$

$$\frac{d}{d\phi_p} \check{v}(z, \omega) = -iW(z)\check{i}(z, \omega) \quad (2)$$

where  $\check{i}(\omega) = \check{I}(\omega)e^{i\omega z/\beta c}$ ,  $\check{v}(\omega) = \check{V}(\omega)e^{i\omega z/\beta c}$ .  $\check{I}(\omega)$ ,  $\check{V}(\omega)$  are the respective Fourier components of the beam current and kinetic-voltage modulations. The kinetic-voltage modulation is related to energy and longitudinal velocity modulations:  $\check{V}(\omega) = -(mc^2/e)\check{\gamma} = -(mc^2/e)\gamma^3\beta\check{\beta}$ ,  $\phi_p(z) = \int_0^z \theta_{pr}(z')dz'$  is the accumulated plasma phase,  $W(z) = r_p^2/(\omega A_e \theta_{pr} \epsilon_0)$  is the beam wave-impedance.  $A_e$  is the effective beam cross-section area,  $\theta_{pr} = r_p \omega_{pl}/\beta c$  is the plasma wavenumber of the Langmuir mode,  $r_p < 1$  is the plasma reduction factor,  $\omega_{pl} = \omega_{po}/\gamma^{3/2}$  is the longitudinal plasma frequency in the laboratory frame. The single-frequency Langmuir plasma wave model expressions [3] can be solved straightforwardly in the case of uniform drift transport. After employing an averaging process, this results in a simple expression for the spectral parameters of stochastic current and velocity fluctuations (noise) in the beam assuming that they are initially uncorrelated[]:

$$\check{i}(L, \omega) = \cos \phi_p(L)\check{i}(0, \omega) + (\sin \phi_p(L)/W_d)\check{v}(0, \omega) \quad (3)$$

where  $\phi_p = \theta_{pr}z$ ,  $\theta_{pr} = r_p \frac{\omega'_p}{v_0}$ ,  $\omega'_p = (\frac{e^2 n_0}{m \epsilon_0 \gamma^3})$ ,  $W_d = \sqrt{\mu_0/\epsilon_0}/k\theta_{pr}A_e$ .

The beam current noise evolution is affected by the initial axial velocity noise through the parameter

$$N^2 = \frac{|\check{v}(0, \omega)|^2/W^2}{|\check{i}(0, \omega)|^2} = (\omega/c\beta k_D)^2 \quad (4)$$

where  $k_D = \omega_{pl}/c\sigma_\beta$  is the Debye wavenumber and  $c\sigma_\beta$  is the axial velocity spread. Equation (4) suggests that current noise suppression is possible if the beam is initially cold  $N^2 < 1$ , and if plasma phase accumulation of  $\phi_p(L) \sim \pi/2$  is feasible.

### NOISE SUPPRESSION EXPERIMENT

The noise suppression demonstration experiment was conducted on the 70 MeV RF-LINAC of ATF/BNL (figure 1). The OTR measurements were carried out at a fixed point (CTR-1) 6.5 m away from the LINAC exit. Keeping the beam spot sizes on viewer YAG4 wide in all experiments made it possible to measure similar OTR image patterns on the CCD screen in all experiments (see figure 3). The measured signal  $S_{OTR}$  was the integrated charge accumulated in all of the pixels of a CCD (charge-coupled device) camera exposed to the OTR emission on the incidence of single electron-beam pulse on the screen. The measured data of  $S_{OTR} = Q_b$  in CTR-0 and CTR-1 are shown in figure 2 as a function of the varied bunch charge  $Q_b$  in the range 200 to 500 pC. The pulse duration in all ex-

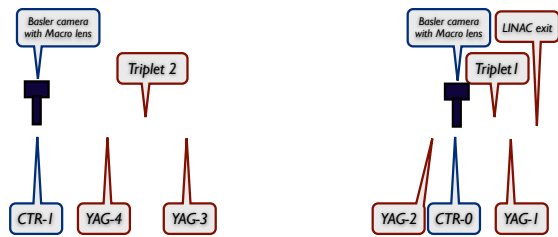


Figure 1: The ATF electron-beam transport set-up is shown from the injector RF-LINAC exit to the OTR viewer site (CTR-1).

periments remained approximately the same (5 ps) corresponding to an average current of 40 to 100A (figure 4). In a shot-noise-dominated beam, in the absence of collective microdynamics, the current noise and consequently  $S_{OTR}$  are proportional to  $I_b$ . Our measured data of  $S_{OTR} = Q_b$  in CTR-0 lie approximately on a horizontal line, confirming the absence of collective microbunching and current-velocity noise correlation or noise suppression before this point. On the other hand, the data measured on CTR-1 exhibit a systematic drop as a function of charge (200 to 500 pC) for all beam energies (50 to 70 MeV). As the measurement conditions at the two measurement positions and at different beam energies could not be made identical, the absolute suppression level between the two points could not be determined. However, the normalized data of all measurements of noise per unit charge depicted in figure 2 show the scaling with charge for all beam energies. This demonstrates attainment of 20 to 30% relative noise suppression, and confirms the predicted effect of collective microdynamic noise suppression process in the drift section.

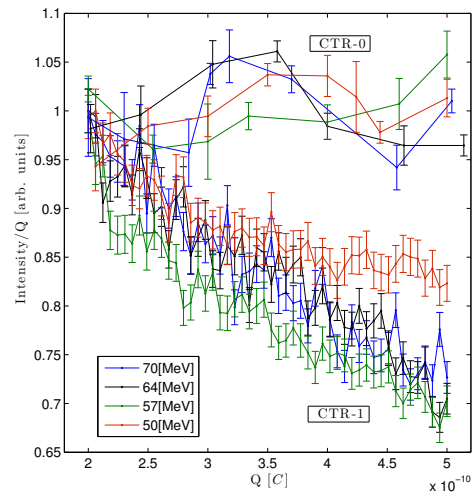


Figure 2: Integrated OTR intensity measurement signals divided by the electron pulse charge. The CTR-1 data correspond to OTR measurement from a screen, intercepting the electron beam 6.5m away from the LINAC exit. The curve's negative slope indicates relative current shot-noise suppression of 20-30% as the beam charge varies from 0.2 to 0.5 nC at different beam energies (50-70 MeV). The CTR-0 data correspond to OTR measurement right after the LINAC exit. Used for reference, its horizontal slope (linear scaling of  $S_{OTR}$  with beam charge) indicates that there was no charge suppression before the collective microdynamic process in the subsequent drift section. The error of the camera integrated signal measurement, 3%, was determined from the variance in the value of the signal due to pulse-to-pulse variation, measured repeatedly while keeping all beam control parameters fixed. The charge measurement error is 1%.

### COMPUTATIONAL MODEL OF COLLECTIVE MICRODYNAMICS IN VARYING CROSS-SECTION BEAM TRANSPORT

At the exit of the Linac, the beam is current-noise dominated, and  $N^2 \ll 1$ . However, due to finite emittance, the axial velocity spread becomes significant as the beam is focused and consequently  $N^2$  (Eq (4)) is no longer negligible. Furthermore, at tight focusing the uniform beam expression (Eq. (3)) cannot be used and in order to calculate the noise suppression, one should solve differential equations for variable beam parameters. In this section we show through a model case computational solution of equations (1) and (2), that the axially varying beam cross section and the excess axial velocity spread due to angular spread can account for a substantial moderation of the noise suppression effect that was realized in the experiment. This example also explains some parameter scaling features of the measurement data.

We turn the generic coupled current and kinetic voltage

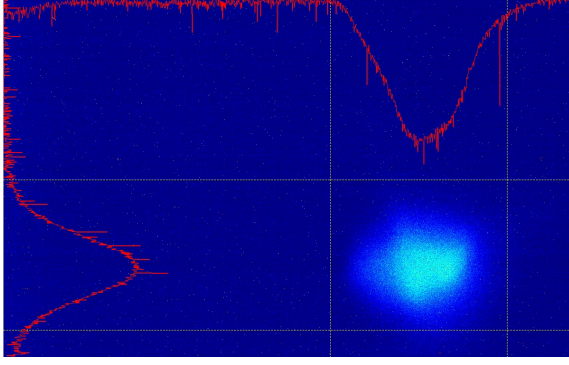


Figure 3: OTR image and axis intensity profiles. Photographed from CTR-1 with a macro lens of 1:1 magnification.

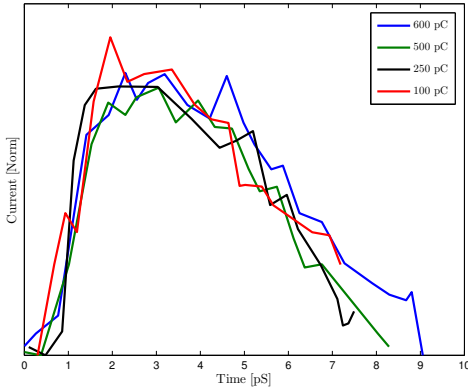


Figure 4: Temporal pulse profile of the e-beam bunch at different bunch charge levels. Pulse duration was approximately 5 pS for all experiments.

equations (1) and (2) into explicit equations in  $z$  by substituting  $\frac{d}{d\phi_p} = \left(\frac{d\phi_p}{dz}\right)^{-1} \frac{d}{dz} = \frac{1}{\phi_{pr}(z)} \frac{d}{dz}$  and  $W(z) = r_p^2 / \omega \epsilon_0 A_e(z) \theta_p(z)$ :

$$\frac{d}{dz} \check{i}(z, \omega) = -i\omega \epsilon_0 A_e(z) \theta_p^2(z) \check{v}(z, \omega) \quad (5)$$

$$\frac{d}{dz} \check{v}(z, \omega) = -\frac{ir_p^2}{\omega \epsilon_0 A_e(z)} \check{i}(z, \omega) \quad (6)$$

where  $\theta_p^2(z) = eZ_0 I_0 / mc^2 A_e(z) \gamma_0^3 \beta_0^3$ .

This set of equations can be solved explicitly numerically if  $A_e(z) = 2\pi\sigma_x(z)\sigma_y(z)$  is given, and the initial conditions  $\check{i}(0, \omega)$ ,  $\check{v}(0, \omega)$  are specified, and the solution at the end of the drift section  $L$  is a linear combination of the initial conditions:  $\check{i}(L, \omega) = A(L)\check{i}(0, \omega) + B(L)\check{v}(0, \omega)$ . Assuming that the current modulation noise and the focusing enhanced velocity noise are uncorrelated at  $z = 0$ , we

set

$$\overline{|\check{i}(L, \omega)|^2} = |A(L)|^2 \overline{|\check{i}(0, \omega)|^2} + |B(L)|^2 \overline{|\check{v}(0, \omega)|^2} \quad (7)$$

$$\overline{|\check{i}(0, \omega)|^2} = eI_b \quad (8)$$

$$\overline{|\check{v}(L, \omega)|^2} = \left(\frac{mc^2}{e} \gamma_0 \beta_0\right)^2 \frac{e}{I_0} \sigma_{\beta z}^2 \quad (9)$$

To compute the noise evolution for the parameters of the reported experiment it is necessary to estimate the cross section dimensions  $\sigma_x(z)$ ,  $\sigma_y(z)$  along the interaction length. This was done based on the measurements on screens YAG-1 to YAG-4, the recorded quad excitation parameters, and performing full 3-D simulation (with space-charge) using GPT.

The beam axial velocity spread due to energy spread ( $\Delta E \simeq 3KeV$ ) is small, and its effect on the initial velocity noise is negligible. We assume that the initial velocity noise is determined by the standard deviation of the axial velocity spread (equation (9)), which was calculated for each quad setting from the angular spread standard deviations due to the focusing and emittance ( $\epsilon_x, \epsilon_y \sim 2-5\mu m$ ):

$$\sigma_{\beta z} = \frac{1}{4}(\sigma_{\beta x}^2 + \sigma_{\beta y}^2) \quad (10)$$

The coefficients  $A(z=L)$ ,  $B(z=L)$  were computed by

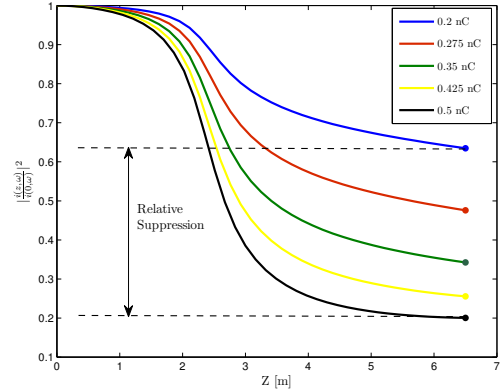


Figure 5: Noise suppression along the collective interaction region as calculated from solution of the coupled differential equations with  $\sigma_x(z)$ ,  $\sigma_y(z)$  of 70 MeV.

iterative integration of the coupled linear differential equations (5 and 6) with the initial conditions ((9)). In Figures 5 and 6 we display the results of the model computation of the variable parameters differential equations. The curves show the noise suppression as function of length and of the beam current for the two extreme energy cases  $E=50$  MeV, 70 MeV. The relative suppression factor in the range  $Q_b=0.2-0.5nC$  at the drift section exit  $L = 6.5m$  is displayed in Fig.(.) for the two beam-energy examples. Figure 7 can only be regarded as a model explanation for the reduced relative noise suppression effect observed in the experiment. As mentioned, there can be additional factors

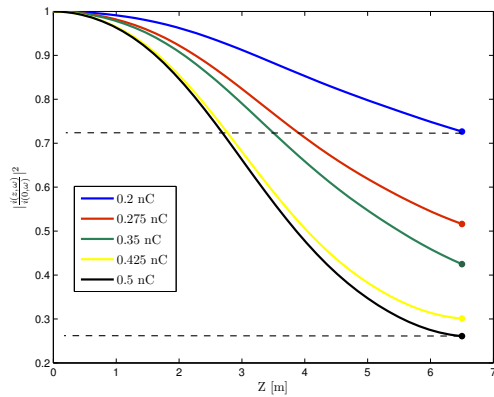


Figure 6: Noise suppression along the collective interaction region as calculated from solution of the coupled differential equations with  $\sigma_x(z)$ ,  $\sigma_y(z)$  of 50 MeV.

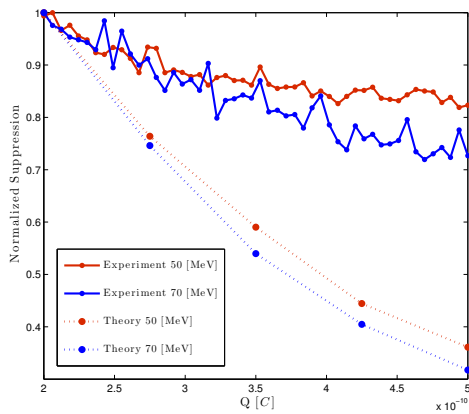


Figure 7: Relative noise suppression rate computed from Eq. 5 and 6 for  $E=50$  MeV, 70 MeV compared to the experimental suppression results.

affecting the suppression rate. It is noted that the computed curves display significantly larger relative suppression in the range  $Q_b=0.2-0.5nC$  than the experimental curves, but in either case there is only little dependence on the acceleration energy. In the simple uniform beam model one would expect dependence of the noise suppression factor on the beam energy due to the  $3/2$  power dependence of the plasma frequency on  $\gamma$ , which corresponds to smaller plasma phase accumulation at higher beam energy. However, the beam envelope had to be varied in the experiment in different beam energies, and one must keep in mind, that at the higher energy the beam focuses into a tighter waist due to the reduced space charge effect. This tends then to increase the plasma frequency at the waist, where most of the microdynamic process takes place.

This observation is consistent with the point of view that the beam envelope expansion and the beam charge homogenization process are in essence the same process of

excess charge beam expansion when viewed in the beam rest frame (independent of the acceleration energy). This is consistent with the plasma phase accumulation theorem of constant plasma phase accumulation in a space charge dominated beam waist [3]. This provides qualitative physical explanation for the weak dependence of the relative noise suppression on the beam energy in the 50-70 MeV range, as depicted in both the experimental (figure 2) and model calculation (figure 7) curves.

## REFERENCES

- [1] A. Gover, A. Nause, E. Dyunin, Beating the shot-noise limit, Nature Physics, doi:10.1038/nphys2443.
- [2] Dicke, R. H., "Coherence in Spontaneous Radiation Processes", Phys. Rev. 93 99–110 (1954).
- [3] A. Gover, E. Dyunin, Collective-Interaction Control and Reduction of Optical Frequency Shot Noise in Charged-Particle Beams, Phys. Rev. Lett. 102, 15 (2009).
- [4] A. Nause, E. Dyunin, "Optical frequency shot-noise suppression in electron beams: Three-dimensional analysis", Journal of App. Phys. 107, 103101 (2010).
- [5] D. Ratner et al, "Observation of Shot Noise Suppression at Optical Wavelengths in a Relativistic Electron Beam", Phys. Rev Lett. 109, 3 (2012).
- [6] Loos, H. and et al, "Observation of coherent optical transition radiation in the LCLS linac", Proceedings of the 2008 Free-Electron Laser Conference (Gyeongju, Korea).
- [7] A. Gover, T. Duchovni, E. Dyunin, A.Nause, "Collective microdynamics and noise suppression in dispersive electron beam transport", Physics of Plasmas 18 123102, (2011).